

# Confocal pH imaging of microscopic specimens using fluorescence lifetimes and phase fluorometry: influence of parameter choice on system performance

K. CARLSSON\*, A. LILJEBORG\*†, R. M. ANDERSSON‡ & H. BRISMAR‡

\*Biomedical & X-Ray Physics, The Royal Institute of Technology, SE-100 44 Stockholm, Sweden

†Physics of Nanostructures, The Royal Institute of Technology, SE-100 44 Stockholm, Sweden

‡Paediatric Unit, Department of Woman and Child Health, Astrid Lindgren Children's Hospital, SE-171 76 Stockholm, Sweden

**Key words.** Confocal microscopy, fluorescence lifetime imaging, pH measurements.

## Summary

We investigate the performance of confocal pH imaging when using phase fluorometry and fluorophores with pH-dependent lifetimes. In these experiments, the specimen is illuminated by a laser beam, whose intensity is sinusoidally modulated. The lifetime-dependent phase shift in the fluorescent signal is detected by a lock-in amplifier, and converted into a pH value through a calibration procedure. A theoretical investigation is made of how the different system parameters will influence the results concerning sensitivity and noise. Experiments carried out with the fluorophore SNAFL-2 support these theoretical predictions. It is found that, under realistic experimental conditions, we can expect a pH change of 0.1 units to be easily detected in an 8-bit digital image. However, the pixel-to-pixel root mean square noise is often of the order of one pH unit. This comparatively high level of noise has its origin in photon quantum noise. pH measurements on living cells show a systematic deviation from expected values. This discrepancy appears to be the result of fluorophore interaction with various cell constituents, and is the subject of further investigation.

## 1. Introduction

In a fluorescence lifetime image, the pixel values represent the fluorescence lifetime at different locations in the object (Lakowicz *et al.*, 1992a). An interesting property of many

fluorophores is that they change their lifetimes in response to the chemical environment. This makes it possible to use lifetime imaging to record, for example, the pH or calcium ion distribution in a specimen (Lakowicz *et al.*, 1992b; Lakowicz & Szmacinski, 1993; Krishnamoorthy & Srivastava, 1997). Recently, there has been a great interest in fluorescence lifetime imaging in microscopy. This is reflected in a number of publications, including those on widefield microscopy (Morgan *et al.*, 1990; Gadella *et al.*, 1993; Oida *et al.*, 1993; Gadella *et al.*, 1994; Squire & Bastiaens, 1999), confocal microscopy (Buurman *et al.*, 1992; van der Oord *et al.*, 1995; Müller *et al.*, 1996; Brismar & Ulvhake, 1997; Buist *et al.*, 1997; Carlsson & Liljeborg, 1998; Sauer *et al.*, 1998) and two-photon microscopy (Piston *et al.*, 1992; So *et al.*, 1995; König *et al.*, 1996; French *et al.*, 1997; Sytsma *et al.*, 1998).

Both time domain and frequency domain methods can be used to record lifetime images. In time domain methods the fluorescence intensity decay after pulse illumination is recorded. In frequency domain methods the specimen is illuminated by intensity-modulated light, and the phase-shift or demodulation of the fluorescent light is studied. Both methods have been used for microscopic imaging. Lifetime imaging techniques have a number of potential advantages compared with techniques based on light intensity measurements. Thus, they avoid problems due to variations in fluorophore concentration, photo-bleaching and light absorption in the specimen (Srivastava & Krishnamoorthy, 1997). Although intensity-ratioing techniques can overcome many of these problems, they still require cumbersome intracellular calibration (Opitz *et al.*, 1995; Sanders *et al.*, 1995). It seems, however, that pH imaging based on fluorescence lifetime could be possible without such intracellular calibration (Sanders *et al.*,

Correspondence: Kjell Carlsson, Biomedical and X-Ray Physics, The Royal Institute of Technology, SE-100 44 Stockholm, Sweden. Tel: + 46 8790 7293; fax: + 46 8 20 56 09; e-mail: kjell@biox.kth.se

1995). Instead, simple buffer solutions could then be used as references.

In this paper we investigate the performance of lifetime imaging of pH, when using confocal microscopy and phase fluorometry. After describing the experimental set-up, we describe the measurement procedure and how the different parameters of the system are selected. We also investigate the sensitivity to pH variations, as well as the noise level in the recorded pH images. Finally, we test this pH imaging method on living cells.

## 2. Experimental set-up

The experimental set-up is shown in Fig. 1. Light from an argon ion laser (Coherent Innova-70, Palo Alto, CA), emitting at 488 nm, illuminates the fluorescent specimen via the photo tube of a microscope (Zeiss Universal, Oberkochen, Germany). The laser light is intensity-modulated at 23 MHz by an electro-optic modulator (EOM; Model 380, Conoptics, Danbury, CT, U.S.A.). Two scanning mirrors (only one is shown in the figure) deflect the laser beam in two perpendicular directions. The fluorescent light from the specimen is descanned by the same mirrors, producing a stationary spot in the plane of the confocal aperture. A photomultiplier tube (PMT; Hamamatsu R1463, Tokyo, Japan) detects the fluorescent light, and the signal from the PMT is connected to a dual-phase lock-in amplifier (a modified PAR 100, Palo Alto Research, CA, U.S.A.), which is phase-locked to the EOM. A more detailed description of the detection principle is given in Carlsson *et al.* (1994) and Carlsson & Liljeborg (1997). Experiments with up to three

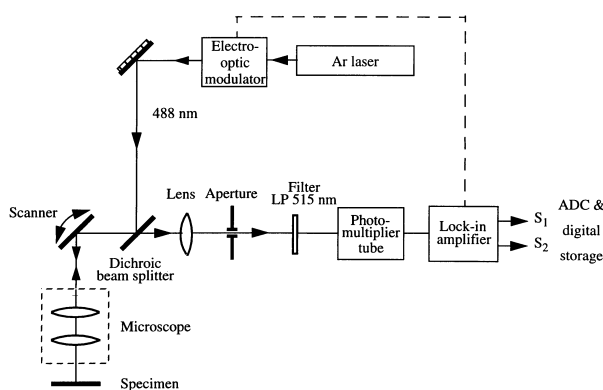


**Fig. 1.** Experimental set-up for confocal pH imaging using fluorescence lifetime. The specimen is illuminated by 488 nm laser light, which is modulated at 23 MHz by an electro-optic modulator. Fluorescent light from the specimen is focused onto a confocal aperture and detected by a photomultiplier tube. A lock-in amplifier, which is phase-locked to the electro-optic modulator, detects the output signal from the photomultiplier tube. If the specimen is labelled with a fluorophore whose lifetime depends on pH, it is possible to calculate specimen pH from the output signals of the lock-in amplifier.

laser wavelengths and three detection channels have been performed for multiple-fluorophore separation (Patwardhan & Manders, 1996; Andersson *et al.*, 1998; Bergman *et al.*, 1999). Simultaneous lifetime imaging of multiple fluorophores has also been carried out with this technique (Carlsson & Liljeborg, 1998). The technique therefore has the potential to simultaneously record multiple ion sensitive probes, although this has not been done in the present study.

Fluorescence lifetime imaging can be performed by utilizing the fact that when a fluorophore is excited by a sinusoidally modulated light source, the fluorescent light will also be sinusoidally modulated, but delayed by a phase angle  $\phi$  compared with the excitation light. Assuming a single-exponential decay, the angle  $\phi$  is given by (Spencer & Weber, 1969)

$$\phi = \text{atan}(\omega\tau) \quad (1)$$

where  $\omega = 2\pi f$ ,  $f$  is the modulation frequency of the excitation light and  $\tau$  is the fluorescence lifetime. In addition to this phase shift, the modulation of the fluorescent light is reduced by a factor of  $m$  compared with that of the exciting light, where

$$m = \frac{1}{\sqrt{1 + \omega^2\tau^2}} \quad (2)$$

The lifetime of the fluorescence can be obtained from either phase shift  $\phi$  or modulation factor  $m$ . In our experiments only the phase shift was used.

When scanning a fluorescent specimen with the set-up shown in Fig. 1, the signals from the two lock-in amplifier outputs are given by (Carlsson & Liljeborg, 1998)

$$S_1 = \frac{I_0 a_0}{2\sqrt{1 + \omega^2\tau^2}} \cdot \cos(\alpha_1 + \phi) \quad (3)$$

$$S_2 = \frac{I_0 a_0}{2\sqrt{1 + \omega^2\tau^2}} \cdot \cos(\alpha_2 + \phi) \quad (4)$$

where  $I_0$  denotes the fluorescence light intensity for the image pixel under consideration,  $a_0$  is the degree of modulation for the excitation light, and  $\phi$  is given by Eq. (1). Phase angles  $\alpha_1$  and  $\alpha_2$  can be varied by using controls on the lock-in amplifier. In commercial dual-phase lock-in amplifiers  $\alpha_2 - \alpha_1$  is usually fixed at  $90^\circ$ , but in our set-up it can be adjusted to any desired value. Forming the ratio,  $R$ , of signals  $S_1$  and  $S_2$ , we get

$$R = \frac{S_1}{S_2} = \frac{\cos(\alpha_1 + \phi)}{\cos(\alpha_2 + \phi)} \quad (5)$$

The phase angle  $\phi$ , and thereby the lifetime  $\tau$ , can be calculated from  $R$  provided that  $\alpha_1$  and  $\alpha_2$  are known (and  $\alpha_1 \neq \alpha_2$ ). This technique for lifetime measurements has previously been described in Carlsson & Liljeborg (1998).

### 3. pH imaging using fluorescence lifetimes

In this study we have used the fluorophore SNAFL-2 (Molecular Probes Europe BV, The Netherlands). SNAFL-2 is a member of a family of fluorophores developed for intensity-ratiometric determination of, for example, pH or  $\text{Ca}^{2+}$  concentration (Grynkiewicz *et al.*, 1985; Haugland, 1996). The ratiometric technique is based on changes in excitation or emission spectra of a fluorophore as a result of changes in the chemical environment. In fact, what happens is that one gets a change in the relative abundance of two populations of fluorophore (protonated and deprotonated in the case of pH) that have different spectral properties. In addition to spectral differences, ratiometric fluorophores may also display lifetime differences for the two populations. This is the case for SNAFL-2, and we will denote the lifetimes of the two populations by  $\tau_1$  and  $\tau_2$ . An interesting property of lifetime measurements of pH, compared with intensity ratio measurements, is that, at least for some fluorophores, it seems possible to avoid cumbersome intracellular calibrations (Sanders *et al.*, 1995).

When using the set-up shown in Fig. 1 to record a multiple-lifetime fluorophore, like SNAFL-2, we get results that are similar to the results for a single-lifetime fluorophore. This means that the fluorescent light will be sinusoidally modulated and phase-shifted, as well as demodulated, compared with the excitation light. Using the phase shift or demodulation to calculate a lifetime value, i.e. using Eqs (1) or (2), will in this case give a weighted average of  $\tau_1$  and  $\tau_2$ . The weight factors will depend on the relative abundance of the two populations of fluorophore (and hence on pH in the case of SNAFL-2). However, the calculated average lifetime value will depend on whether phase shift or demodulation data are used. We denote these values  $\tau_\phi$  and  $\tau_m$ , respectively. It is possible to determine both  $\tau_1$  and  $\tau_2$ , as well as their relative amplitudes, by making recordings of  $\tau_\phi$  or  $\tau_m$  at three different modulation frequencies. This is not necessary, however, if the objective is to measure pH rather than  $\tau_1$  and  $\tau_2$ . In fact, it is not necessary to calculate any lifetime values at all. Instead one can record the ratio value  $R$  in Eq. (5), and use a calibration procedure to find a direct relationship between  $R$  and pH. We have adopted this technique, because it facilitates the measurement procedure. When using the ratio  $R$ , only the phase shift (and not the demodulation) is utilized. Consequently, the only lifetime of interest in the following text is  $\tau_\phi$ . For convenience we will from now on simply denote this by  $\tau$ , with the understanding that what is actually meant is  $\tau_\phi$ .

### 4. Choice of parameters

The choice of angles  $\alpha_1$  and  $\alpha_2$  will influence the ratio value  $R$  in Eq. (5). It is therefore natural to ask how these angles

should be selected for best results. There are several factors to take into account. First, we prefer that none of the signals  $S_1$  and  $S_2$  goes negative; one reason for this is that the values are stored in a digital image memory, another is that sign changes are potentially dangerous when forming ratio values. Second, noise should be as low as possible given the number of detected photons. Third, we must get sufficient sensitivity, i.e. a biologically interesting change in pH must give a change in  $R$  that is easily detected. The conditions necessary to fulfil these requirements will be addressed separately below. We will also calculate the optimum modulation frequency, and investigate the expected performance when doing pH measurements. In summary, the results show that non-negativity and sufficient sensitivity can be easily obtained. The expected noise level is of the order of one pH unit.

#### 4.1. Non-negative output signals

From Eqs (3) and (4) we see that  $S_1$  and  $S_2$  will be positive if

$$-\frac{\pi}{2} < \alpha_n + \phi < \frac{\pi}{2}, \quad n = 1, 2 \quad (6)$$

As we have seen, it is necessary that  $\alpha_1 \neq \alpha_2$ , and in the following discussion we shall assume that  $\alpha_1 < \alpha_2$ . If, in response to varying pH, the lifetime of the fluorescence,  $\tau$ , varies between  $\tau_{\min}$  and  $\tau_{\max}$ , Eq. (6) can only be satisfied if

$$\alpha_1 > -\frac{\pi}{2} - \phi_{\min} \text{ and } \alpha_2 < \frac{\pi}{2} - \phi_{\max} \quad (7)$$

where  $\phi_{\min} = \text{atan}(\omega\tau_{\min})$  and  $\phi_{\max} = \text{atan}(\omega\tau_{\max})$ . In practice,  $\alpha_2 - \alpha_1$  is set to a fixed value before the experiments begin, and both angles are then adjusted together by a single control. From Eq. (7) we see that the angular difference  $\alpha_2 - \alpha_1$  must fulfil the condition

$$\alpha_2 - \alpha_1 < \pi - \phi_{\max} + \phi_{\min} \quad (8)$$

As we shall later see, a large value for  $\alpha_2 - \alpha_1$  gives a high sensitivity to pH variations. Since  $0 < \phi < \frac{\pi}{2}$  (corresponding to lifetimes between zero and infinity), we can handle all possible lifetimes if  $\alpha_2 - \alpha_1 \leq \frac{\pi}{2}$ . If, on the other hand,  $\alpha_2 - \alpha_1 \geq \pi$ , we can handle no lifetime variations at all. For SNAFL-2 the lifetime varies approximately from 1 to 4 ns. With a modulation frequency of 23 MHz, which was used in our experiments, the maximum allowed value for  $\alpha_2 - \alpha_1$  is approximately 160°. This means, however, that for lifetimes close to 1 or 4 ns we get output signals close to zero. The choice of  $\alpha_2 - \alpha_1$  will be further discussed in section 4.3, where the sensitivity is investigated.

After selecting a value for  $\alpha_2 - \alpha_1$ , there is only one free angular parameter to set. Under practical image recording conditions, the easiest procedure, and the one we have used, is to set this angle so that the brightest parts of the  $S_1$  and  $S_2$  images have similar intensities (this can be easily done by

using a pseudocolour scale during image scanning). If this is done we get

$$\alpha_2 + \phi_{\min} = -\alpha_1 - \phi_{\max} \quad (9)$$

The above result is obtained from Eqs (3), (4) and (7), provided that  $\alpha_1 < \alpha_2$ . With an angular setting according to Eq. (9), also the darkest parts of the  $S_1$  and  $S_2$  images will have equal intensities. Furthermore, this minimum intensity will be maximized, i.e. we have done our best to avoid pixel values close to zero. As will be shown below, the choice of angles  $\alpha_1$  and  $\alpha_2$  does not affect the noise in the pH images.

#### 4.2. Noise in pH measurements

Noise in the output signals from the lock-in amplifier will introduce a statistical variation in time of the ratio value  $R$ . This noise will propagate into the pixel values of the pH image. The root mean square (RMS) noise in the pH measurements,  $\sigma_{\text{pH}}$ , is given by:

$$\sigma_{\text{pH}} = \lim_{T \rightarrow \infty} \sqrt{\frac{1}{T} \int_0^T (\text{pH}_{\text{meas}} - \text{pH})^2 dt} \quad (10)$$

where the variable  $t$  represents time,  $\text{pH}_{\text{meas}}$  is the measured value, which is influenced by noise, and  $\text{pH}$  represents the value we would measure in the absence of noise. As in previous investigations of noise (Carlsson, 1995; Carlsson & Liljeborg, 1997; Carlsson & Liljeborg, 1998), we assume that photon quantum noise strongly dominates. This has proved to be a good approximation in the experiments carried out. To calculate  $\sigma_{\text{pH}}$  from Eq. (10), we make the assumption that fluorescence lifetime is a linear function of pH in the region of interest. This was considered sufficient at the present stage of the investigations, where the aim was to estimate the influence of many different parameters rather than a careful analysis of individual parameters. Furthermore, the linear model is a reasonable approximation within a limited pH range, as can be seen from published data on SNARF-1 (Srivastava & Krishnamoorthy, 1997) and SNAFL-2 (Liljeborg *et al.*, 1998). We therefore write

$$\text{pH} = k_1 \cdot \tau + k_2 \quad (11)$$

where  $k_1$  and  $k_2$  are constants. Inserting this linear relationship into Eq. (10) we get

$$\sigma_{\text{pH}} = |k_1| \left( \lim_{T \rightarrow \infty} \sqrt{\frac{1}{T} \int_0^T (\tau_{\text{meas}} - \tau)^2 dt} \right) = |k_1| \cdot \sigma_{\tau} \quad (12)$$

where  $\sigma_{\tau}$  denotes the RMS lifetime noise, which was calculated in Carlsson & Liljeborg (1998). Using the results from this previous study, we get the following expression for  $\sigma_{\text{pH}}$

$$\sigma_{\text{pH}} = |k_1| \cdot \frac{\sqrt{2}(1 + (\omega\tau)^2)^{3/2}}{a_0 \sqrt{\bar{N}} \omega} \quad (13)$$

where  $\bar{N}$  is the average number of detected photons per pixel, and  $\tau$  is the lifetime we would measure in the absence of noise. Not surprisingly, we see that  $\sigma_{\text{pH}}$  is reduced by detecting many photons per pixel and by using a high degree of modulation for the excitation light. We also note that the angles  $\alpha_1$  and  $\alpha_2$  do not influence  $\sigma_{\text{pH}}$ . Therefore, these angles can be selected without considering the noise.

If the angular frequency for the light modulation,  $\omega$ , can be selected at will,  $\sigma_{\text{pH}}$  is minimized by setting  $\omega = 1/\sqrt{2}\tau$ . We then get

$$\sigma_{\text{pH,min}} = \frac{3.67|k_1|\tau}{a_0 \sqrt{\bar{N}}} = \frac{3.67|(\text{pH} - k_2)|}{a_0 \sqrt{\bar{N}}} \quad (14)$$

In addition to the number of detected photons, and the degree of light modulation,  $\sigma_{\text{pH,min}}$  also depends on pH value and the relationship between fluorescence lifetime and pH (Eq. 11). To get some typical  $\sigma_{\text{pH,min}}$  values for real experimental situations, we used published data on the pH-sensitive fluorophores SNARF-1 (Srivastava & Krishnamoorthy, 1997) and SNAFL-2 (Liljeborg *et al.*, 1998). The useful pH range is approximately 5.5–8 for SNARF-1, and 5–9 for SNAFL-2. Estimating curve parameter  $k_2$  from the approximately linear central part of the published curves, and using Eq. (14), we get for SNARF-1

$$\sigma_{\text{pH,min}} = \frac{3.67|(\text{pH}_{\text{true}} - 4.5)|}{a_0 \sqrt{\bar{N}}} \quad (15)$$

and for SNAFL-2

$$\sigma_{\text{pH,min}} = \frac{3.67|(\text{pH}_{\text{true}} - 9.8)|}{a_0 \sqrt{\bar{N}}} \quad (16)$$

It would seem from Eqs (15) and (16) that we could perform noise-free measurements at pH values 4.5 and 9.8 with the two fluorophores. This is not true, of course, as the values for curve parameter  $k_2$  used in Eqs (15) and (16) are valid only for a pH approximately in the range 6.1–7.1 for SNARF-1 and 7.5–9.0 for SNAFL-2 (in other pH regions other values for  $k_2$  must be used). For pH values near the middle of the valid pH ranges, we get  $\sigma_{\text{pH,min}}$  values of approximately  $8/(a_0 \sqrt{\bar{N}})$  for SNARF-1 and  $6/(a_0 \sqrt{\bar{N}})$  for SNAFL-2. If the excitation light has 50% modulation, and an average of 100 photons are detected per pixel,  $\sigma_{\text{pH}}$  will be of the order of 1–1.5 pH units. Even if the number of photons is increased to 1000, which is a lot in confocal fluorescence microscopy,  $\sigma_{\text{pH}}$  will be nearly half a pH unit.

The fact that the optimum modulation frequency depends on fluorescence lifetime (which in turn depends on pH) gives practical difficulties. It means that when recording the pH distribution in a specimen, we would have to vary the frequency in a manner not known beforehand. In addition, the optimum frequency may be unattainable for technical reasons (or the modulation may be too low at this frequency). In our present set-up we use 23 MHz, although the optimum frequency is in the range 30–110 MHz for

SNAFL-2. This means that  $\sigma_{\text{pH}}$  will be larger by a factor of up to 2.8 compared with the optimum choice of frequency. Figure 2 shows  $\sigma_{\text{pH}}$ , calculated from Eq. (13), as a function of modulation frequency and pH for SNAFL-2. A linear relationship between pH and  $\tau$  (Eq. 11) was assumed.

#### 4.3. Sensitivity to pH variations

In the previous section we saw that pH images will be rather noisy unless the photon count is very high. It is therefore doubtful if a high sensitivity to pH variations is useful. Nevertheless, we shall look at the general problem of what possibilities exist for the choice of sensitivity.

We define the relative sensitivity,  $S$ , for pH measurements as  $S = 1/R \cdot |dR/d(\text{pH})|$ , where  $R$  is the signal ratio defined by Eq. (5). We chose to look at the relative, rather than absolute, sensitivity because the former is independent of the magnitude of the ratio value  $R$ . This magnitude is of little interest because it will be influenced by, for example, amplification factors and image scaling. In the final image the digital values are usually scaled to fit into a suitable range of integer numbers, e.g. 0–255 for an 8-bit image.

$S$  depends on three things. First, it depends on how the ratio  $R$  varies with the phase angle  $\phi$ . Second, it depends on how  $\phi$  varies with lifetime  $\tau$ . Third, it depends on how the lifetime varies with pH. We can therefore write  $S$  as

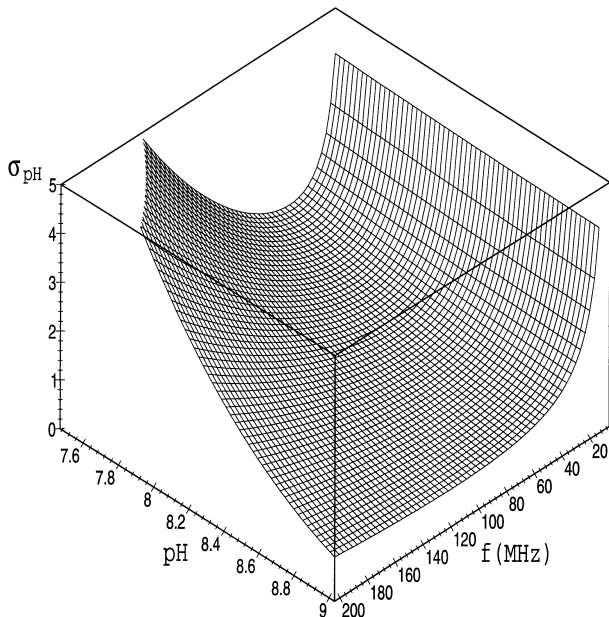


Fig. 2. Root mean square (RMS) noise in pH measurements,  $\sigma_{\text{pH}}$ , as a function of modulation frequency and pH. Data shown are theoretical values for the fluorescent pH probe SNAFL-2, assuming that the average number of detected photons per pixel is 100 and that the excitation light has a modulation of 50%.

$$S = \frac{1}{R} \cdot \left| \frac{dR}{d\phi} \cdot \frac{d\phi}{d\tau} \cdot \frac{d\tau}{d(\text{pH})} \right| \quad (17)$$

The value for  $1/R \cdot dR/d\phi$  depends on angles  $\alpha_1$  and  $\alpha_2$ , whereas the other factors do not. It is therefore sufficient to study how  $\alpha_1$  and  $\alpha_2$  will affect  $1/R \cdot dR/d\phi$ . Furthermore, we have seen that  $\alpha_1$  and  $\alpha_2$  will not affect the noise. This means that we can select these angles so that we get the desired sensitivity, as long as the non-negativity constraint for signals  $S_1$  and  $S_2$  is fulfilled. Using Eq. (5), we get

$$\frac{1}{R} \cdot \frac{dR}{d\phi} = \frac{\sin(\alpha_2 - \alpha_1)}{\cos(\alpha_1 + \phi)\cos(\alpha_2 + \phi)} \quad (18)$$

The value for  $1/R \cdot dR/d\phi$  depends not only on  $\alpha_1$  and  $\alpha_2$  but also on  $\phi$  (which is equal to  $\text{atan}(\omega\tau)$ ). It can be mathematically proven that the function in Eq. (18) increases monotonously as a function of  $\alpha_2 - \alpha_1$  for all lifetimes if Eq. (9) is satisfied. Therefore, the general conclusion is that larger values for  $\alpha_2 - \alpha_1$  give higher sensitivity in detecting pH variations. This is exemplified in Fig. 3, where  $1/R \cdot dR/d\phi$  is plotted as a function of  $\alpha_2 - \alpha_1$  for a number of different lifetimes. In all experiments we selected  $\alpha_2 - \alpha_1 = \pi/2$ , because this is guaranteed to work for all fluorescence lifetimes, and also prevents the output signals from becoming too small. As will be shown below, this setting also gives a sufficiently high sensitivity for pH measurements.

We will now investigate the other factors in Eq. (17). Taking the derivative of Eq. (1) we get  $d\phi/d\tau = \omega/(1 + (\omega\tau)^2)$ , and from Eq. (11) we get  $d\tau/d(\text{pH}) = 1/k_1$ . Combining these results with Eqs (9) and (18), and setting  $\alpha_2 - \alpha_1 = \pi/2$ , we get

$$S = \left| \frac{2}{\cos(2\phi - \phi_{\max} - \phi_{\min})} \cdot \frac{\omega}{1 + \tan^2\phi} \cdot \frac{1}{k_1} \right| \quad (19)$$

The value of  $S$  depends on the angular frequency of the excitation light,  $\omega$ , which should be set to  $1/\sqrt{2}\tau$  to minimize noise. To get an idea of what  $S$ -values to expect in a real situation, we used previously recorded data for SNAFL-2 (Liljeborg *et al.*, 1998). These data showed that when the pH value varies between 6 and 9, the measured lifetime varies between approximately 3.4 and 1.0 ns. From Eq. (13) it is clear that the highest noise level is obtained for the longest lifetime. In order to make this noise value as low as possible, we should use a modulation frequency of 33 MHz. For this frequency we calculated the expected average  $S$ -values in different pH regions using Eq. (19), and the results are presented in Table 1. Also listed in Table 1 are the expected values for a frequency of 23 MHz, which was used in our experiments (this was the highest frequency attainable in our set-up). From the values in Table 1 it is possible to calculate that for a pH change of 0.1 units, we can expect a change in an 8-bit digital ratio image of at least

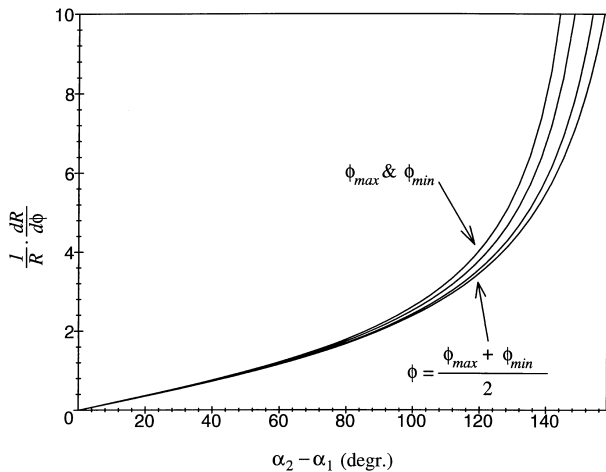


**Fig. 3.** Sensitivity factor  $1/R \cdot dR/d\phi$  as a function of the phase angle setting  $\alpha_2 - \alpha_1$  of the lock-in amplifier (see text for details). The different curves represent different  $\phi$  values, and thus different fluorescence lifetimes ( $\phi = \text{atan}(\omega\tau)$ ). To obtain a range of possible  $\phi$  values, it was assumed that the fluorescence lifetime varies between 1 ns and 4 ns in response to pH variations. It was also assumed that the excitation light was modulated at 23 MHz. This situation resembles the actual experimental conditions for our experiments with SNAFL-2. It is clear that a high sensitivity to pH variations can be obtained by using large values for  $\alpha_2 - \alpha_1$ . However, the maximum value is limited to  $158^\circ$  in the current case, because of the demand for positive output signals from the lock-in amplifier. In fact we used  $\alpha_2 - \alpha_1 = 90^\circ$  in all experiments, which gives  $1/R \cdot dR/d\phi \approx 2$ . This sensitivity turns out to be quite sufficient, and guarantees that, under all experimental conditions, we can obtain positive pixel values in the recorded images.

two to three levels. This sensitivity should be quite sufficient considering the noise level in the measurements (probably at least 0.5 pH units, as described in section 4.2). From these estimates we conclude that sufficient sensitivity can easily be attained with the described settings for  $\alpha_1$  and  $\alpha_2$ , even when data are stored as 8-bit numbers.

## 5. Experiments

To investigate the relative sensitivity,  $S$ , and the noise,  $\sigma_{\text{pH}}$ , we used a specimen manufactured from four glass capillary

**Table 1.** Theoretically predicted sensitivity,  $S$ , to pH variations.  $S = 1/R \cdot |dR/d(\text{pH})|$ , where  $R = S_1/S_2$ , see Fig. 1.

pH range	$f = 33 \text{ MHz}$ (minimum noise)	$f = 23 \text{ MHz}$ (frequency used)
6–7.4	0.14	0.11
7.4–8	0.41	0.32
8–9	0.40	0.29

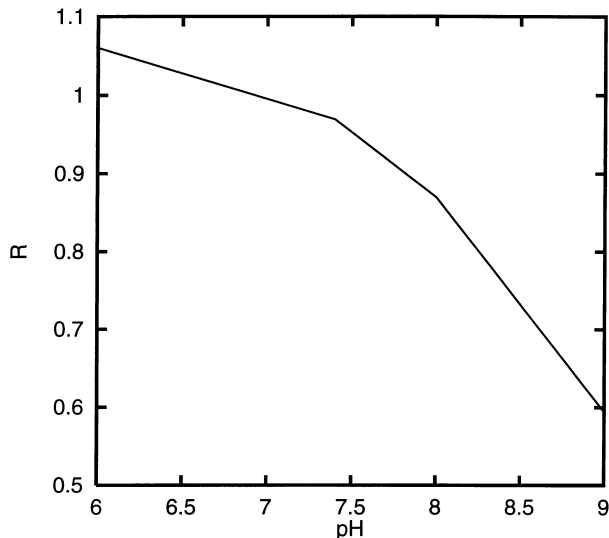


**Fig. 4.** Example of a calibration curve, relating ratio values  $R = S_1/S_2$  (see Fig. 1) to pH values. The curve is based on measurements from the capillary reference specimen described in the text.

tubes, each with a diameter of 0.2 mm. The tubes were filled with buffer solutions of pH 6, 7.4, 8 and 9. SNAFL-2 (free acid) was added to the buffer solutions to give a concentration of  $30 \mu\text{M}$  of the probe. The ends of the tubes were then sealed, and the tubes were mounted side-by-side on an object glass. This specimen was scanned with a 10/0.32 objective, which allowed all four capillaries to be imaged simultaneously within the field of view of the microscope. The sensitivity and noise figures obtained from these recordings were compared with theoretical predictions.

To get some experience of biological specimens, we used macrophages prepared from rat lung and plated on glass the day before use. The cells were loaded in a physiological salt solution containing  $30 \mu\text{M}$  of cell membrane permeable SNAFL-2 AM ester for 1 h at room temperature. After scanning the cell preparations, the capillary specimen described above was scanned using the same instrument settings (except for the objective). From the capillary recordings, a calibration curve was produced which related the ratio values  $R$  to pH values. An example of such a calibration curve is

**Table 2.** RMS noise in pH measurements ( $f = 23 \text{ MHz}$ . Approx. 1000 detected photons per pixel).

pH	$\sigma_{\text{pH}}$ theoretical	$\sigma_{\text{pH}}$ experimental
6	1.9	1.8
7.4	1.1	1.2
8	0.7	1.0

seen in Fig. 4. Using this curve, we converted pixel ratio values from the cell images into pH values.

### 5.1. Measurements of relative sensitivity and noise

Values for relative sensitivity,  $S$ , were extracted from a

calibration curve like the one shown in Fig. 4. For the three pH regions 6–7.4, 7.4–8 and 8–9, we obtained average  $S$ -values of 0.09, 0.20 and 0.29. Comparing these numbers with the estimates in Table 1 we see a fairly good agreement, except for the pH region 7.4–8 where the value is a bit low.

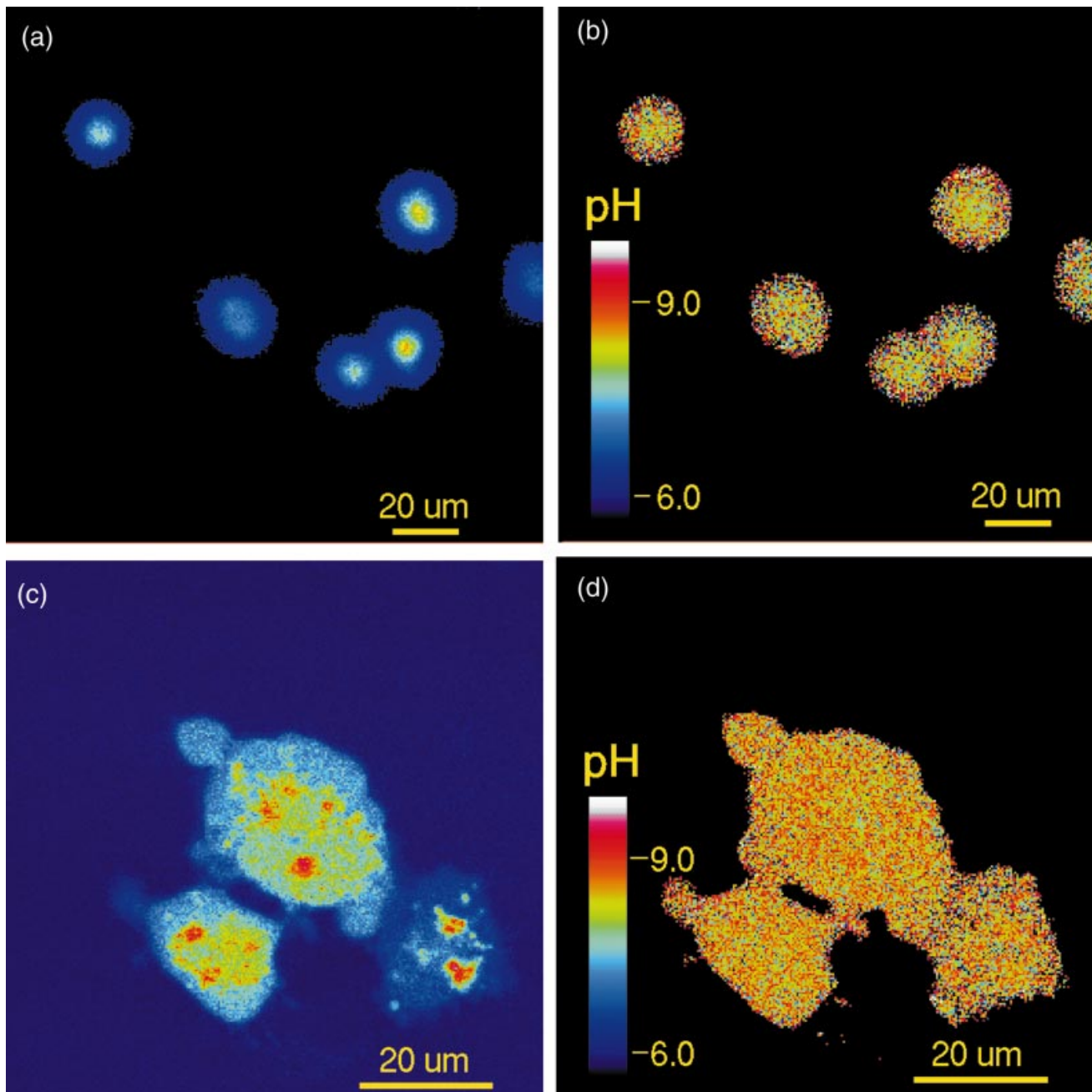


**Fig. 5.** Images of living cells. (a) Raw data image of macrophages from rat lung. The pixel values were recorded from one of the lock-in amplifier outputs ( $S_1$ ,  $S_2$ ) in Fig. 1. Pseudo-colours are used to illustrate different signal levels. (b) pH image of macrophages. A ratio image ( $S_1/S_2$ ) was formed, and the ratio values were converted to pH using a calibration curve similar to the one shown in Fig. 4. To exclude areas with low pixel values (e.g. background) a threshold was applied before computing the ratio values. Those areas are displayed in black. (c) Raw data image of COS-7 cells (monkey kidney cell line). (d) pH image of COS-7 cells. All cells were loaded with SNAFL-2 AM ester, and recorded with the instrument shown in Fig. 1.

Investigations of the noise were made by calculating the standard deviation in ratio images of the capillaries. In this way we obtained the experimental  $\sigma_{\text{pH}}$  values listed in Table 2. To compare these  $\sigma_{\text{pH}}$  values with theory, using Eq. (13), we needed values for  $|k_1|$  and  $a_0\sqrt{N}$ . Values for  $|k_1|$  could be estimated from data given in Liljeborg *et al.* (1998), and estimates of  $a_0\sqrt{N}$  were obtained from noise measurements in the intensity images  $S_1$  and  $S_2$  used for calculating the ratio  $R$ . We excluded pH 9 because of difficulties in estimating a value for  $|k_1|$  in this pH region. The theoretical estimates for  $\sigma_{\text{pH}}$  thus obtained are also listed in Table 2, and they agree rather well with the measured values.

### 5.2. pH imaging of living cells

Image scanning of living macrophages was done with a 63/1.2 water immersion objective (Fig. 5a,b). From the recorded data we obtained an average intracellular pH of entire cells of  $8.11 \pm 0.08$  ( $n = 6$ ). This is higher than the normal pH of 7.2 found in the cytoplasm. Besides a higher value, the pH was also practically constant throughout the whole cell (Fig. 5b). Similar results have previously been obtained with cultivated COS-7 cells (Liljeborg *et al.*, 1998), an example of which is given in Fig. 5(c,d). However, when using the same microscope objective and instrument settings to scan a buffer solution rather than living cells, we obtained pH values that were close to the correct values (within 0.2–0.3 pH units). Possible explanations for this discrepancy are discussed in the next section.

## 6. Discussion

In this study we have investigated the performance of confocal pH imaging based on fluorescence lifetimes and phase fluorometry. We have made theoretical predictions concerning sensitivity and noise, which have been supported by experimental results.

When scanning living cells the results were not as expected. Macrophages were chosen for pH imaging because of their well known production of vesicles called phagosomes, which have low internal pH (4–6). Besides these, mitochondria and peroxisomes would be expected to give a spatial pH difference inside the cell. However, apart from noise, our pH measurements only recorded a nearly homogeneous pH inside the cells. Such homogeneous pH images of cells have also been reported by another group (Sanders *et al.*, 1995). A possible explanation for these results is that more than two fluorophore populations exist due to fluorophore interaction with, for example, proteins inside a cell (Srivastava & Krishnamoorthy, 1997). If this is the case, erroneous pH values may be produced. We have recently carried out some experiments to see to what extent fluorophore interaction with various cell constituents can influence pH measurements based on average fluorescence

lifetimes (Andersson *et al.*, 2000). It turns out that the pH measurements can indeed be strongly influenced by proteins and lipids. This effect can be so large (corresponding to more than two pH units in some cases) that it could strongly mask the pH variations inside a cell. Different fluorophores behave differently in this respect, however, which could explain why Sanders *et al.* (1995) did not encounter any major problem of this sort. If fluorophore interaction with cell constituents turns out to be a major problem, it is possible to extend the described phase fluorometry technique to measurements at multiple modulation frequencies. This opens the possibility to resolve multi-exponential decay characteristics, and thereby possibly avoid the problem of fluorophore interaction with cell constituents. This possibility has been demonstrated in time-domain measurements by Srivastava & Krishnamoorthy (1997).

## Acknowledgements

This work has been financially supported by the Swedish Research Council for Engineering Sciences, Carl Trygger Foundation and Anders Wall Foundation.

## References

- Andersson, R.M., Carlsson, K., Liljeborg, A. & Brismar, H. (2000) Fluorescence lifetime imaging of pH in cells: investigation of factors influencing the pH calibration lifetime. *Proc. SPIE*, **3921**, 242–248.
- Andersson, T., Patwardhan, A., Emilson, A., Carlsson, K. & Scheynius, A. (1998) HLA-DM is expressed on the cell surface and colocalizes with HLA-DR and invariant chain in human Langerhans cell. *Arch. Dermatol. Res.* **290**, 674–680.
- Bergman, E., Carlsson, K., Liljeborg, A., Manders, E., Hökfelt, T. & Ulfhake, B. (1999) Neuropeptides, nitric oxide synthase and GAP-43 in B4-binding and RT97 immunoreactive primary sensory neurons: normal distribution pattern and changes after peripheral nerve transection and aging. *Brain Res.* **832**, 63–83.
- Brismar, H. & Ulfhake, B. (1997) Fluorescence lifetime measurements in confocal microscopy of neurons labeled with multiple fluorophores. *Nature Biotechnol.* **15**, 373–377.
- Buist, A.H., Müller, M., Gijsbers, E.J., Brakenhoff, G.J., Sosnowski, T.S., Norris, T.B. & Squier, J. (1997) Double-pulse fluorescence lifetime measurements. *J. Microsc.* **186**, 212–220.
- Buurman, E.P., Sanders, R., Draaijer, A., Gerritsen, H.C., van Veen, J.J.F., Houpt, P.M. & Levine, Y.K. (1992) Fluorescence lifetime imaging using a confocal laser scanning microscope. *Scanning*, **14**, 155–159.
- Carlsson, K. (1995) Signal-to-noise ratio for confocal microscopy when using the Intensity-modulated Multiple-beam Scanning (IMS) technique. *Micron*, **26**, 317–322.
- Carlsson, K., Åslund, N., Mossberg, K. & Philip, J. (1994) Simultaneous confocal recording of multiple fluorescent labels with improved channel separation. *J. Microsc.* **176**, 287–299.

- Carlsson, K. & Liljeborg, A. (1997) Confocal fluorescence microscopy using spectral and lifetime information to simultaneously record four fluorophores with high channel separation. *J. Microsc.* **185**, 37–46.
- Carlsson, K. & Liljeborg, A. (1998) Simultaneous confocal lifetime imaging of multiple fluorophores using the intensity-modulated multiple-wavelength scanning (IMS) technique. *J. Microsc.* **191**, 119–127.
- French, T., So, P.T.C., Weaver, D.J., Coelho-Sampaio, T. & Gratton, E. (1997) Two-photon fluorescence lifetime imaging microscopy of macrophage-mediated antigen processing. *J. Microsc.* **185**, 339–353.
- Gadella, T.W.J., Clegg, R.M. & Jovin, T.M. (1994) Fluorescence lifetime imaging microscopy: pixel-by-pixel analysis of phase-modulation data. *Bioimaging*, **2**, 139–159.
- Gadella, T.W.J., Jovin, T.M. & Clegg, R.M. (1993) Fluorescence lifetime imaging microscopy (FLIM): spatial resolution of microstructures on the nanosecond timescale. *Biophys. Chem.* **48**, 221–239.
- Grynkiewicz, G., Poenie, M. & Tsien, R.Y. (1985) A new generation of  $\text{Ca}^{2+}$  indicators with greatly improved fluorescence properties. *J. Biol. Chem.* **260**, 3440–3450.
- Haugland, R.P. (1996) *Handbook of Fluorescent Probes and Research Chemicals*. Molecular Probes, Inc, Eugene, OR, U.S.A.
- König, K., So, P.T.C., Mantulin, W.W., Tromberg, B.J. & Gratton, E. (1996) Two-photon excited lifetime imaging of autofluorescence in cells during UVA and NIR photostress. *J. Microsc.* **183**, 197–204.
- Krishnamoorthy, G. & Srivastava, A. (1997) Intracellular dynamics seen through time-resolved fluorescence microscopy. *Curr. Sci.* **72**, 835–845.
- Lakowicz, J.R. & Szmacinski, H. (1993) Fluorescence lifetime-based sensing of pH,  $\text{Ca}^{2+}$ ,  $\text{K}^+$  and glucose. *Sens. Act. B*, **11**, 133–143.
- Lakowicz, J.R., Szmacinski, H., Nowaczkyk, K., Berndt, K.W. & Johnson, M. (1992a) Fluorescence lifetime imaging. *Anal. Biochem.* **202**, 316–330.
- Lakowicz, J.R., Szmacinski, H., Nowaczkyk, K. & Johnson, M.L. (1992b) Fluorescence lifetime imaging of calcium using Quin-2. *Cell Calcium*, **13**, 131–147.
- Liljeborg, A., Carlsson, K. & Andersson, R.M. (1998) Fluorescence lifetime imaging of multiple fluorophores implemented in confocal microscopy. *Proc. SPIE*, **3568**, 82–88.
- Morgan, C.G., Mitchell, A.C. & Murray, J.G. (1990) Nanosecond time-resolved fluorescence microscopy: principles and practice. *Trans. Roy. Microsc. Soc.* **1**, 463–466.
- Müller, R., Zander, C., Sauer, M., Deimel, M., Ko, D.-S., Siebert, S., Arden-Jacob, J., Deltau, G., Marx, N.J., Drexhage, K.H. & Wolfrum, J. (1996) Time-resolved identification of single molecules in solution with a pulsed semiconductor diode laser. *Chem. Phys. Lett.* **262**, 716–722.
- Oida, T., Sako, Y. & Kusumi, A. (1993) Fluorescence lifetime imaging microscopy (flimscopy). *Biophys. J.* **64**, 676–685.
- van der Oord, C.J.R., Gerritsen, H.C., Rommerts, F.F.G., Shaw, D.A., Munro, I.H. & Levine, Y.K. (1995) Micro-volume time-resolved fluorescence spectroscopy using a confocal synchrotron radiation microscope. *Appl. Spectrosc.* **49**, 1469–1473.
- Opitz, N., Merten, E. & Acker, H. (1995) Local intracellular ion measurements with luminescent indicators using confocal laser scanning microscopy. *Proc. SPIE*, **2508**, 90–101.
- Patwardhan, A. & Manders, E.M.M. (1996) Three-colour confocal microscopy with improved colocalization capability and cross-talk suppression. *Bioimaging*, **4**, 17–24.
- Piston, D.W., Sandison, D.R. & Webb, W.W. (1992) Time-resolved fluorescence imaging and background rejection by two-photon excitation in laser scanning microscopy. *Proc. SPIE*, **1640**, 379–389.
- Sanders, R., Draaijer, A., Gerritsen, H.C., Houpt, P.M. & Levine, Y.K. (1995) Quantitative pH imaging in cells using confocal fluorescence lifetime imaging microscopy. *Anal. Biochem.* **227**, 302–308.
- Sauer, M., Arden-Jacob, J., Drexhage, K.H., Göbel, F., Lieberwirth, U., Mühllegger, K., Müller, R., Wolfrum, J. & Zander, C. (1998) Time-resolved identification of individual mononucleotide molecules in aqueous solution with pulsed semiconductor lasers. *Bioimaging*, **6**, 14–24.
- So, P.T.C., French, T., Yu, W.M., Berland, K.M., Dong, C.Y. & Gratton, E. (1995) Time-resolved fluorescence microscopy using two-photon excitation. *Bioimaging*, **3**, 49–63.
- Spencer, R.D. & Weber, G. (1969) Measurements of subnanosecond fluorescence lifetimes with a cross-correlation phase fluorometer. *Ann. NY Acad. Sci.* **158**, 361–376.
- Squire, A. & Bastiaens, P.I.H. (1999) Three dimensional image restoration in fluorescence lifetime imaging microscopy. *J. Microsc.* **193**, 36–49.
- Srivastava, A. & Krishnamoorthy, G. (1997) Time-resolved fluorescence microscopy could correct for probe binding while estimating intracellular pH. *Anal. Biochem.* **249**, 140–146.
- Sytsma, J., Vroom, J.M., de Grauw, C.J. & Gerritsen, H.C. (1998) Time-gated fluorescence lifetime imaging and microvolume spectroscopy using two-photon excitation. *J. Microsc.* **191**, 39–51.